


## AUTHOR QUERY FORM

	<b>Journal:</b> ENSM  <b>Article Number:</b> 6	<b>Please e-mail your responses and any corrections to:</b>  <b>E-mail:</b> <a href="mailto:corrections.esch@elsevier.macipd.com">corrections.esch@elsevier.macipd.com</a>
---	--	--

Dear Author,

Please check your proof carefully and mark all corrections at the appropriate place in the proof (e.g., by using on-screen annotation in the PDF file) or compile them in a separate list. Note: if you opt to annotate the file with software other than Adobe Reader then please also highlight the appropriate place in the PDF file. To ensure fast publication of your paper please return your corrections within 48 hours.

For correction or revision of any artwork, please consult <http://www.elsevier.com/artworkinstructions>.

Any queries or remarks that have arisen during the processing of your manuscript are listed below and highlighted by flags in the proof. Click on the [Q](#) link to go to the location in the proof.

Your article is registered as a regular item and is being processed for inclusion in a regular issue of the journal. If this is NOT correct and your article belongs to a Special Issue/Collection please contact [v.sethuraman@elsevier.com](mailto:v.sethuraman@elsevier.com) immediately prior to returning your corrections.

Location in article	Query / Remark: <a href="#">click on the Q link to go</a> Please insert your reply or correction at the corresponding line in the proof
<a href="#">Q1</a>	Please confirm that given names and surnames have been identified correctly and are presented in the desired order.
<a href="#">Q2</a>	Figures [1] have been submitted as color images; however, the captions have been reworded to ensure that they are meaningful when your article is reproduced both in color and in black and white. Please confirm if the changes made are ok.
<a href="#">Q3</a>	Reference(s) given here were noted in the reference list but are missing from the text – please position each reference in the text or delete it from the list.

Thank you for your assistance.

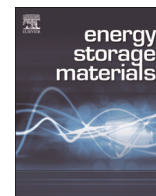
Please check this box or indicate your approval  
if you have no corrections to make to the PDF file



ELSEVIER

Contents lists available at ScienceDirect

## Energy Storage Materials

journal homepage: [www.elsevier.com/locate/ensm](http://www.elsevier.com/locate/ensm)

## Graphical Abstract

## Pseudocapacitance of zeolite-templated carbon in organic electrolytes

Khanin Nueangnoraj<sup>a</sup>, Hirotomo Nishihara<sup>a</sup>, Takafumi Ishii<sup>a</sup>, Norihisa Yamamoto<sup>a</sup>,  
 Hiroyuki Itoi<sup>b</sup>, Raúl Berenguer<sup>c</sup>, Ramiro Ruiz-Rosas<sup>d</sup>, Diego Cazorla-Amorós<sup>d</sup>,  
 Emilia Morallón<sup>c</sup>, Masashi Ito<sup>e</sup>, Takashi Kyotani<sup>a</sup>

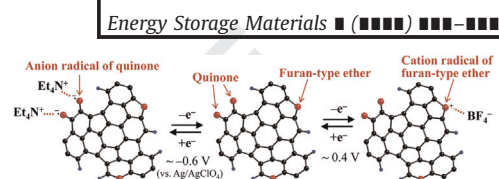
<sup>a</sup> Institute of Multidisciplinary Research for Advanced Materials, Tohoku University, 2-1-1 Katahira, Aoba, Sendai 980-8577, Japan

<sup>b</sup> Department of Applied Chemistry, Faculty of Engineering, Aichi Institute of Technology, 1247 Yachigusa, Yakusa, Toyota 470-0392, Japan

<sup>c</sup> Departamento de Química Inorgánica e Instituto Universitario de Materiales, Universidad de Alicante, Apdo. 99, Alicante, Spain

<sup>d</sup> Departamento de Química Física e Instituto Universitario de Materiales, Universidad de Alicante, Apdo. 99, Alicante, Spain

<sup>e</sup> Advanced Materials Laboratory, Nissan Research Center, Nissan Motor Co. Ltd., 1 Natsushima-cho, Yokosuka-shi, Kanagawa 237-8523, Japan

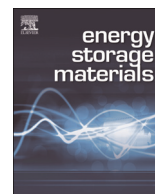




ELSEVIER

Contents lists available at ScienceDirect

## Energy Storage Materials

journal homepage: [www.elsevier.com/locate/ensm](http://www.elsevier.com/locate/ensm)

## Pseudocapacitance of zeolite-templated carbon in organic electrolytes

Khanin Nueangnoraj<sup>a</sup>, Hirotomo Nishihara<sup>a,\*</sup>, Takafumi Ishii<sup>a</sup>, Norihisa Yamamoto<sup>a</sup>, Hiroyuki Itoi<sup>b</sup>, Raúl Berenguer<sup>c</sup>, Ramiro Ruiz-Rosas<sup>d</sup>, Diego Cazorla-Amorós<sup>d</sup>, Emilia Morallón<sup>c</sup>, Masashi Ito<sup>e</sup>, Takashi Kyotani<sup>a</sup>

<sup>a</sup> Institute of Multidisciplinary Research for Advanced Materials, Tohoku University, 2-1-1 Katahira, Aoba, Sendai 980-8577, Japan

<sup>b</sup> Department of Applied Chemistry, Faculty of Engineering, Aichi Institute of Technology, 1247 Yachigusa, Yakusa, Toyota 470-0392, Japan

<sup>c</sup> Departamento de Química Inorgánica e Instituto Universitario de Materiales, Universidad de Alicante, Apdo. 99, Alicante, Spain

<sup>d</sup> Departamento de Química Física e Instituto Universitario de Materiales, Universidad de Alicante, Apdo. 99, Alicante, Spain

<sup>e</sup> Advanced Materials Laboratory, Nissan Research Center, Nissan Motor Co. Ltd., 1 Natsushima-cho, Yokosuka-shi, Kanagawa 237-8523, Japan

## ARTICLE INFO

## Article history:

Received 7 July 2015

Received in revised form

21 August 2015

Accepted 21 August 2015

## ABSTRACT

Carbon and graphene-based materials often show some amount of pseudocapacitance due to their oxygen-functional groups. However, such pseudocapacitance is generally negligible in organic electrolytes and has not attracted much attention. In this work, we report a large pseudocapacitance of zeolite-templated carbon (ZTC) based on the oxygen-functional groups in 1 M tetraethylammonium tetrafluoroborate dissolved in propylene carbonate (Et<sub>4</sub>NBF<sub>4</sub>/PC). Due to its significant amount of active edge sites, a large amount of redox-active oxygen functional groups are introduced into ZTC, and ZTC shows a high specific capacitance (330 F g<sup>-1</sup>). Experimental results suggest that the pseudocapacitance could be based on the formation of anion and cation radicals of quinones and ethers, respectively. Moreover, ZTC shows pseudocapacitance also in 1 M lithium hexafluorophosphate dissolved with a mixture of ethylene carbonate and diethyl carbonate (LiPF<sub>6</sub>/EC+DEC) which is used for lithium-ion batteries and lithium-ion capacitors.

© 2015 Published by Elsevier B.V.

## 1. Introduction

Towards the development of high-energy pseudocapacitors and hybrid capacitors, various types of redox-based active materials have been investigated, e.g. conductive polymer [1,2], organic compounds [3–7], and metal oxides [8,9]. The conductivities of these active materials are generally not sufficient, and therefore, they are usually mixed with conductive additives. However, this results in low mass-fraction of the redox-active materials. In addition, the redox active materials are generally not durable for long-term use, and most of them are redox-active only in aqueous electrolytes, which further limits their applications. It would be ideal if conductive carbon materials themselves could exhibit a large pseudocapacitance, especially in organic electrolytes having a wide potential window (ca. 3V).

We have recently reported that zeolite-templated carbon (ZTC), an ordered microporous carbon prepared by using zeolite as a hard template [10,11], has a very large amount of active edge sites, namely ca. 10 times larger than the amount of ordinary activated carbons. Moreover, such edge sites can be easily functionalized by

a large amount of quinone groups in H<sub>2</sub>SO<sub>4</sub> electrolyte [12,13]. The quinone groups give rise to high pseudocapacitance (ca. 500 F g<sup>-1</sup>) with reasonably high rate capability and good cyclability [13]. In this work, we report the introduction of redox-active oxygen functional groups to ZTC in tetraethylammonium tetrafluoroborate dissolved in propylene carbonate (Et<sub>4</sub>NBF<sub>4</sub>/PC). The edge sites of ZTC are so active that the functional groups are easily introduced even within a potential range which is too narrow for general carbon materials to be electrochemically-reacted. The oxygen functional groups thus introduced in ZTC show a large pseudocapacitance at two different potentials in the organic electrolyte. We then try to understand the origin of the pseudocapacitance. Moreover, we examine the behavior of ZTC in lithium hexafluorophosphate dissolved with a mixture of ethylene carbonate and diethyl carbonate (LiPF<sub>6</sub>/EC+DEC) to see if ZTC exhibits pseudocapacitance in the different type of organic electrolyte.

## 2. Experimental

ZTC was prepared using the method reported elsewhere [14]. ZTC is characterized by a very large BET surface area of 3600 m<sup>2</sup> g<sup>-1</sup> as well as by ordered micropores with a uniform size of 1.2 nm.

\* Corresponding author. Tel.: +81 22 217 5627; fax: +81 22 217 5626.

E-mail address: [nishihara@tagen.tohoku.ac.jp](mailto:nishihara@tagen.tohoku.ac.jp) (H. Nishihara).

<http://dx.doi.org/10.1016/j.ensm.2015.08.003>

2405-8297/© 2015 Published by Elsevier B.V.

A three-electrode cell was constructed inside a glove box (Ar atmosphere). An electrode sheet for a working electrode was prepared by mixing ZTC, PTFE, and carbon black with the weight ratio of 90:5:5. About 10 mg of the electrode sheet was sandwiched by a Pt mesh to form the working electrode. Using the same manner, a counter electrode was also prepared, but an activated carbon fiber (Unitika, A20) was used instead of ZTC. The working electrode was isolated from a counter electrode by a cellulose separator. A reference electrode consisted of Ag/AgClO<sub>4</sub>. The electrochemical characterization was carried out using the three-electrode cell with 1 M Et<sub>4</sub>NBF<sub>4</sub>/PC at 25 °C, in a fixed potential range from -1.5 to 1.0 V to clarify the mechanisms of electrochemical oxidation of ZTC and the appearance of pseudocapacitance. For comparison, two types of commercial activated carbons (Kansai Coke and Chemicals Co., Ltd., MSC30; Kuraray Chemical Co., Ltd., YP-50F) were used as reference. MSC30 is a KOH-activated carbon having a large BET surface area of 2680 m<sup>2</sup> g<sup>-1</sup>. YP-50F is a steam-activated carbon which is indeed used as an electrode material of commercial electric double-layer capacitors. YP-50F has a BET surface area of 1700 m<sup>2</sup> g<sup>-1</sup>, and is highly durable for long-term use.

By the electrochemical oxidation [13], quinone-functionalized ZTC was also prepared and characterized to elucidate the effect of quinone-type oxygen functional groups (see Supporting information about the details of this experiment).

In order to understand the effect of the electrochemical oxidation on the carbon surface chemistry, some of electrode sheets before and after the electrochemical characterizations were analyzed by temperature-programmed desorption (TPD) [15] and FT-IR (Shimadzu, FTIR-8900) [13]. For these analyses, the electrode sheet taken out from the current collector was washed by acetone with sonication for 30 min. Then, the washed sample was separated from the acetone by filtration. The sonication and filtration were repeated twice and the sample was finally dried at 80 °C under reduced pressure for 6 h.

The stable potential range of ZTC was also examined by the following method. First, cyclic voltammetry (CV) was performed for 4 cycles in a narrow potential range of -1.5 to 0.5 V (vs Ag/AgClO<sub>4</sub>). Then, galvanostatic charge/discharge cycling (GC) was conducted at several different current densities. Next, the upper limit potential was increased stepwise from 0.5 to 1.3 V, and the set of CV and GC was repeated at each of the potential ranges. Similar potential expansion towards negative potential region was done in the same manner but the upper limit potential was fixed at 0.5 V and the lower limit potential was expanded stepwise from -1.5 to -2.3 V. The stable potential range of ZTC was determined from the change of the specific capacitance or color change of the electrolyte. Then, the electrochemical performance of ZTC was examined in the stable potential range (-2.0 to 1.0 V) determined by the above experiment.

A set of electrochemical measurements was made also in 1 M LiPF<sub>6</sub>/EC+DEC. In this case, stainless mesh was used instead of Pt mesh, and Li foil was used as both reference and counter electrodes.

### 3. Results and discussion

#### 3.1. Pseudocapacitance of ZTC in 1 M Et<sub>4</sub>NBF<sub>4</sub>/PC

Fig. 1a shows cyclic voltammograms of ZTC in 1 M Et<sub>4</sub>NBF<sub>4</sub>/PC. The black and red lines corresponds to the 1st and the 4th scans measured in -1.5 to 1.0 V, respectively. At the initial positive-direction scan (black line), a large anodic current is observed above 0.5 V, and subsequently a redox peak appears around 0.4 V. We have recently reported very similar results of ZTC in an aqueous electrolyte (1 M H<sub>2</sub>SO<sub>4</sub>) [13], i.e., ZTC is intensively oxidized at the first positive-direction scan and a large amount of quinone-type groups

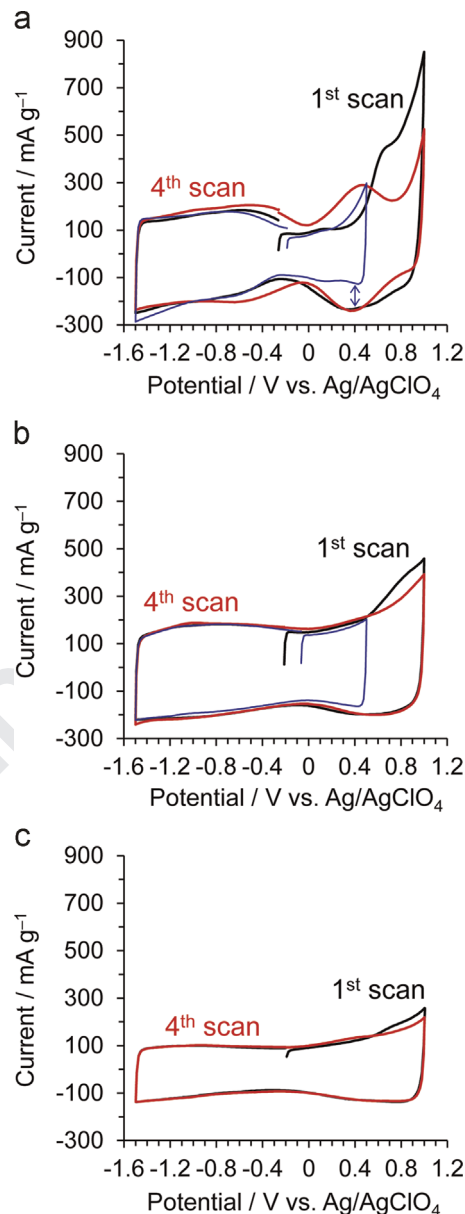


**Fig. 1.** CV patterns of (a) ZTC, (b) MSC30, and (c) YP-50F, measured in 1 M Et<sub>4</sub>NBF<sub>4</sub>/PC at 25 °C. A scan rate is 1 mV s<sup>-1</sup>. The 1st and the 4th CV patterns measured in a potential range from -1.5 to 1.0 V are expressed by black and red lines, respectively, while the 1st CV pattern measured in a potential range from -1.5 to 0.5 V is expressed by a blue line. (For interpretation of the references to color in this figure legend, the reader is referred to the web version of this article.)

are introduced, which gives rise to a large pseudocapacitance. For reference, the 1st scan (blue line) measured in -1.5 V to 0.5 V is also shown in Fig. 1a. It is noteworthy that the blue line shows almost no reduction peak around 0.4 V (indicated by an arrow). Fig. 1a thus indicates that the redox active species are generated during the initial positive-direction scan above 0.5 V. Additionally, another broad and weak redox peak can be observed at a negative potential around -0.6 V in the 4th scan (red line), though this peak is very weak at the 1st negative-direction scan (black line). The corresponding redox active species seems to be different from the origin of the pseudocapacitance around 0.4 V, and they are gradually introduced into ZTC during the four CV cycles.

The aforementioned behavior of ZTC is totally different from those of the commercial activated carbons (Fig. 1b and c), whose voltammograms exhibit a typical rectangular shape based on electric double layer capacitance regardless of the number of cycle.

Thus, the anodic process seen in ZTC would be due to the unique structure of this carbon. It should be noted that Pt, the present current collector, can catalyze the anodic decomposition of PC solvent at a high potential [16]. Fig. 1b and c, however, indicates that such Pt-catalyzed PC decomposition does not occur in the activated carbons at the present potential range. In addition, we have proved that ZTC is also free from such a problem by a separated experiment (Supporting information, Fig. S1).

To investigate the origin of the pseudocapacitance, ZTC after the polarization was subjected to the TPD analysis. During the heating in a TPD run, oxygen functional groups are decomposed to CO and CO<sub>2</sub> gases at different temperatures, depending on their types. It is generally accepted that the decomposition of ethers, phenols, and quinone-type carbonyls results in the desorption of CO, carboxylic groups and lactones give CO<sub>2</sub>, and acid anhydrides produce both CO and CO<sub>2</sub> (molar ratio 1:1) [17–19]. The resulting CO and CO<sub>2</sub> desorption profiles are shown in Fig. 2, and their amounts are summarized in Table 1 together with the total oxygen content. It is found that the amounts of CO and CO<sub>2</sub> desorption from ZTC increase upon the positive polarization up to 1.0 V, indicating that oxygen functional groups are indeed introduced into ZTC by the electrochemical oxidation in 1 M Et<sub>4</sub>NBF<sub>4</sub>/PC. In Fig. 2, major enhancement can be seen in the CO evolution around 400–1000 °C. Since CO<sub>2</sub> evolution is not similarly increased, the large CO evolution in the oxidized ZTC would be mainly derived from ethers, phenols, and/or quinone groups [17–19]. Consequently, one or some of these groups may contribute to the pseudocapacitance. Though a trace amount of H<sub>2</sub>O (< 30 ppm) is contained in the electrolyte solution, we have confirmed that the origin of the oxygen-functional groups is not H<sub>2</sub>O, but PC, by a separated experiment (Supporting information, S3). It has been reported that the present solvent (PC) reacts with many compounds, such as phenol and tiophenol, to form CO<sub>2</sub> and

hydroxyalkyl derivatives including oxygen derived from PC [16,20] at a high potential and the direct reaction of PC with activated carbons is also possible [20]. Since the edge sites of ZTC are electrochemically more active than those of conventional porous carbons [12,13], it is likely that only ZTC can react with PC as shown in Fig. 1 and a large amount of ethers, phenols, and/or quinone groups are introduced as a result.

Since the present electrolyte includes not only oxygen but also nitrogen and boron, it is necessary to consider the possibility of the introduction of other functional groups including these heteroatoms which also exhibit pseudocapacitance [21–23]. However, we have confirmed that functional groups containing nitrogen or boron are not introduced into ZTC by the present polarization condition (see Supporting information, Fig. S4).

### 3.2. Redox reaction in the negative potential range

The next question is which type of oxygen functional group may be responsible for the observed pseudocapacitance. We have recently reported that ZTC can be easily electro-oxidized in H<sub>2</sub>SO<sub>4</sub>, and a large amount of quinone groups can be introduced into ZTC with a high selectivity [13]. Quinones are generally known as redox-active functional groups, which can exhibit pseudocapacitance in

**Table 1**  
Amounts of CO, CO<sub>2</sub>, and H<sub>2</sub>O evolutions and total oxygen content of the pristine ZTC electrode and the one polarized in –1.5 to 1.0 V.

Polarization potential (V)	Amount of gas evolution ( $\mu\text{mol g}^{-1}$ )			Total oxygen content (wt%)
	CO	CO <sub>2</sub>	H <sub>2</sub> O	
Pristine	1624	173	1095	4.9
–1.5 to 1.0	3939	1039	3007	14.4

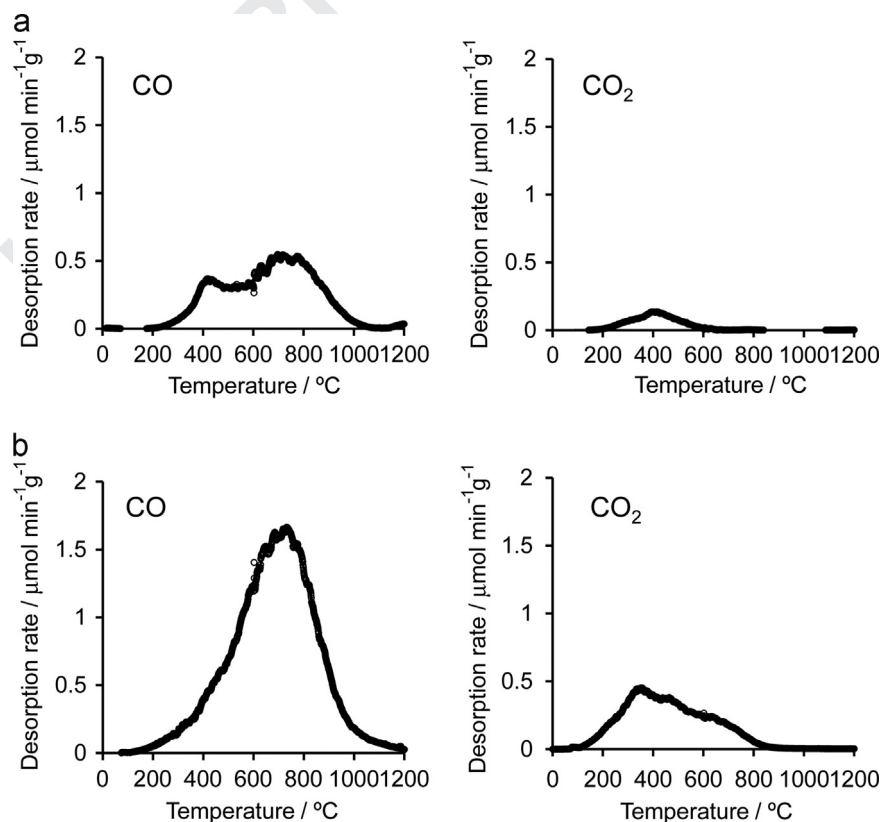


Fig. 2. CO and CO<sub>2</sub> TPD patterns of electrode sheets including ZTC, (a) before and (b) after polarization between –1.5 and 1.0 V.

organic electrolytes [24,25]. Thus, we prepared the quinone-functionalized ZTC, and examined its electrochemical response in 1 M  $\text{Et}_4\text{NBF}_4/\text{PC}$ . The quinone-functionalized ZTC indeed exhibits a couple of intense peaks in a negative potential range (Fig. 3). Quinone groups would therefore correspond to the pseudocapacitance in the negative potential range. The redox potential of quinones in organic molecules varies with the molecular structure and/or with the adjacent functional groups, both of which affect the electron affinity of quinones [25,26]. But, most of the observed potentials stay within the range of the broad peak in Fig. 3.

### 3.3. Redox reaction in the positive potential range

Most of edge sites of the quinone-functionalized ZTC are occupied by quinone groups, and therefore, this sample is not severely oxidized in the initial positive-direction scan (Supporting information, Fig. S4). Besides, the quinone-functionalized ZTC does not show pseudocapacitance in the positive potential range (Fig. 3). Consequently, the origin of the pseudocapacitance cannot be ascribed to quinones, but it may be ethers and/or phenols. In addition, ethers and/or phenols should be introduced at the initial anodic oxidation above 0.5 V.

Fig. S5 shows FT-IR spectra of ZTC before and after the polarization up to 0.7 V. Ethers, phenols, and quinones generally give IR absorption bands at 1000–1300, 3200–3400 and 1600–1900  $\text{cm}^{-1}$  due to C–O, O–H and C=O stretching modes, respectively [27,28]. By the polarization up to 0.7 V, a new peak appears in the region of the C–O stretching, suggesting that the redox peak at 0.4 V (Figs. 1a and 3) corresponds to ethers.

To our best knowledge, a furan ring is the only ether-type group which shows reversible redox reaction in this positive potential range [29]. We thus propose a possible redox reaction scheme of ZTC in 1 M  $\text{Et}_4\text{NBF}_4/\text{PC}$ , as shown in Fig. 4. ZTC is first electrochemically oxidized above 0.4 V (Fig. 1a) with PC, and furan-type ethers are introduced as a result. By the following cycles, in addition to the ethers, redox-active quinones are slowly introduced in ZTC. The

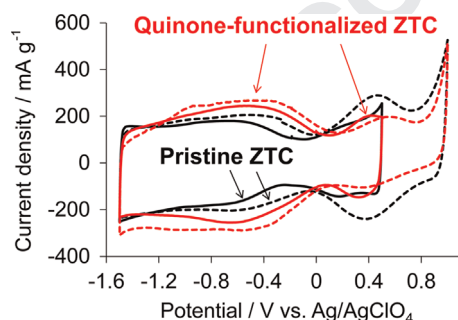


Fig. 3. Cyclic voltammograms (fourth scan) of the pristine ZTC (black lines) and the quinone-functionalized ZTC (red lines), measured in 1 M  $\text{Et}_4\text{NBF}_4/\text{PC}$  up to 0.5 V (solid lines), and 1.0 V (dotted lines). A scan rate is 1  $\text{mV s}^{-1}$ . (For interpretation of the references to color in this figure legend, the reader is referred to the web version of this article.)

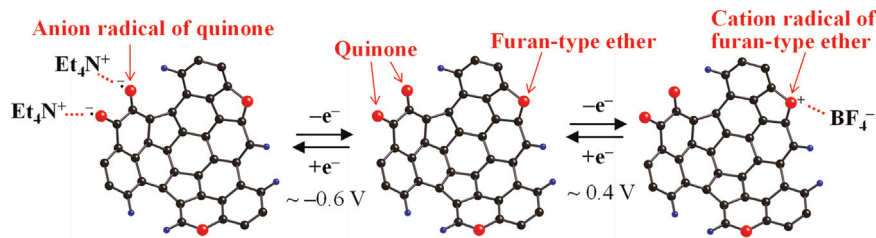


Fig. 4. A possible redox-reaction scheme of oxygen-functionalized ZTC in 1 M  $\text{Et}_4\text{NBF}_4/\text{PC}$ .

former is reversibly oxidized/reduced by the formation of its cation radical [29], and thus shows pseudocapacitance around 0.4 V. The latter is also reversibly oxidized/reduced by the formation of its anion radical [31], and shows pseudocapacitance around  $-0.6$  V.

### 3.4. Stable potential range of ZTC in 1 M $\text{Et}_4\text{NBF}_4/\text{PC}$

Fig. 5 shows the change of capacitance of ZTC and MSC30, when the upper (Fig. 5a) or lower (Fig. 5b) limit potential is expanded to a positive or negative direction, respectively. Electric double-layer capacitance is generally independent of an operating potential. Therefore, in Fig. 5a, MSC30 keeps a constant capacitance (ca. 180  $\text{F g}^{-1}$ ) up to 1.6 V. At a very high potential of 1.8 V, the capacitance is decreased due to the decomposition of electrolyte and the subsequent formation of polymer-like solids which cause the pore blocking [29]. This is a typical result in general porous carbons. By contrast, ZTC shows capacitance enhancement with increasing the upper limit potential up to 1.0 V, due to the development of pseudocapacitance. However, the capacitance

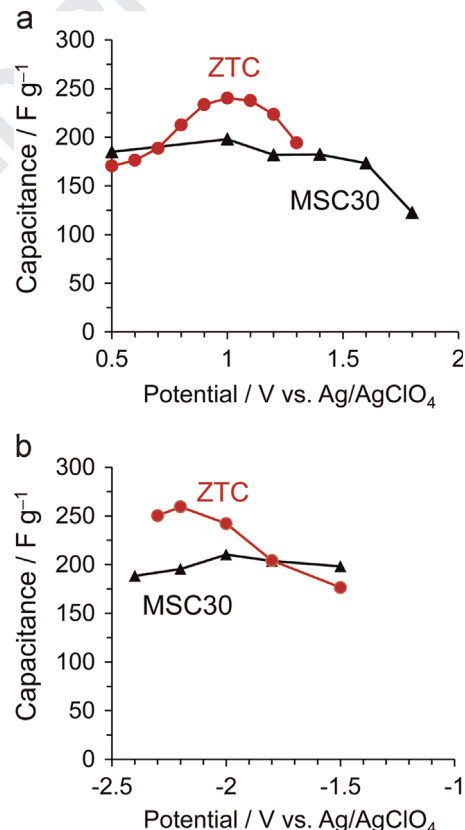
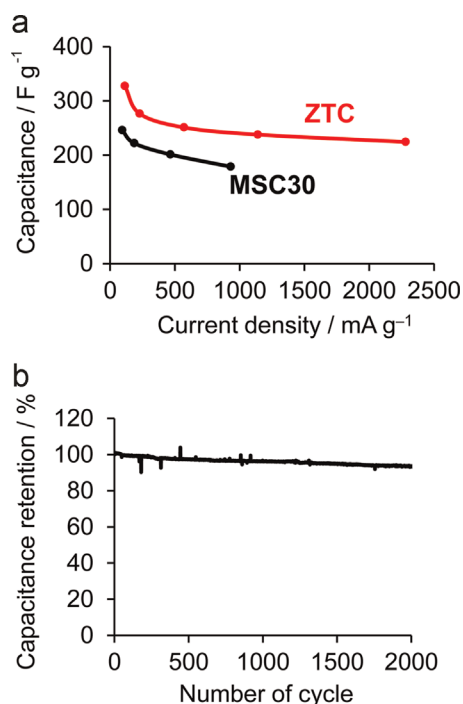


Fig. 5. Capacitance versus (a) lower or (b) upper potential range of GC measurement ( $0.1 \text{ A g}^{-1}$ ) in 1 M  $\text{Et}_4\text{NBF}_4/\text{PC}$  for ZTC and MSC30. The potential range was expanded stepwise from 0.5 V to more positive range in the case of (a), and from  $-1.5$  V to more negative range in the case of (b).



**Fig. 6.** (a) Capacitance versus current density for ZTC and MSC30, measured between  $-2.0$  and  $1.0$  V in  $1$  M Et<sub>4</sub>NBF<sub>4</sub>/PC. (b) Durability test of ZTC upon 2000 charge/discharge cycles, measured at  $1$  A g<sup>-1</sup> in  $1$  M Et<sub>4</sub>NBF<sub>4</sub>/PC.

declines above  $1.1$  V, suggesting the formation of polymer-like solids and the subsequent occurrence of pore-blocking. Thus, we conclude that the upper limit of the stable potential range of ZTC in  $1$  M Et<sub>4</sub>NBF<sub>4</sub>/PC is  $1.0$  V.

In the negative potential region (Fig. 5b), the capacitance of MSC30 is stable (ca.  $200$  F g<sup>-1</sup>) down to  $-2.4$  V. On the other hand, ZTC shows capacitance increase down to  $-2.2$  V, followed by a decline at  $-2.3$  V. It should be noted that the color of the electrolyte was however turned into right brown at  $-2.2$  V, indicating the degradation of the electrolyte already at this potential. Therefore, we concluded that the lower limit of the stable potential range of ZTC is  $-2.0$  V.

### 3.5. Rate capability and cycle stability

The rate capability and cycle stability of ZTC are then examined in its stable potential range ( $-2.0$  to  $1.0$  V). By the contribution of pseudocapacitance, ZTC indeed has a higher specific capacitance ( $330$  F g<sup>-1</sup>) than those of YP-50F ( $120$  F g<sup>-1</sup>) and MSC30 ( $250$  F g<sup>-1</sup>) in GC measurement at  $50$  mA g<sup>-1</sup>. Fig. 6a shows capacitance dependence on current density for ZTC and MSC30. Despite the contribution of pseudocapacitance, ZTC retains a high specific capacitance ( $224$  F g<sup>-1</sup>) at a large current density of  $2280$  mA g<sup>-1</sup>, and its rate performance is as good as that of MSC30. The good rate performance suggests that (1) the framework of ZTC is not severely destroyed [13], and (2) ZTC is free from pore-blocking by the deposition of polymer-like layers. Besides, we have proved that electro-oxidation of ZTC allows the introduction of a large amount of oxygen-functional groups with retaining its high specific surface area [12]. In addition, the ZTC retains 94% of its initial capacitance after 2000 cycles of charge/discharge measurements (Fig. 6b). These results prove that the redox-active functional groups introduced into ZTC are stable and can repeat the fast redox reactions reversibly thousands of times in the determined potential range ( $-2.0$  to  $1.0$  V).

It should be noted that the potential range of ZTC ( $-2.0$  to  $1.0$  V) is actually narrower than that of MSC30 ( $-2.4$  to  $1.6$  V), and ZTC is not advantageous for constructing high-energy symmetric

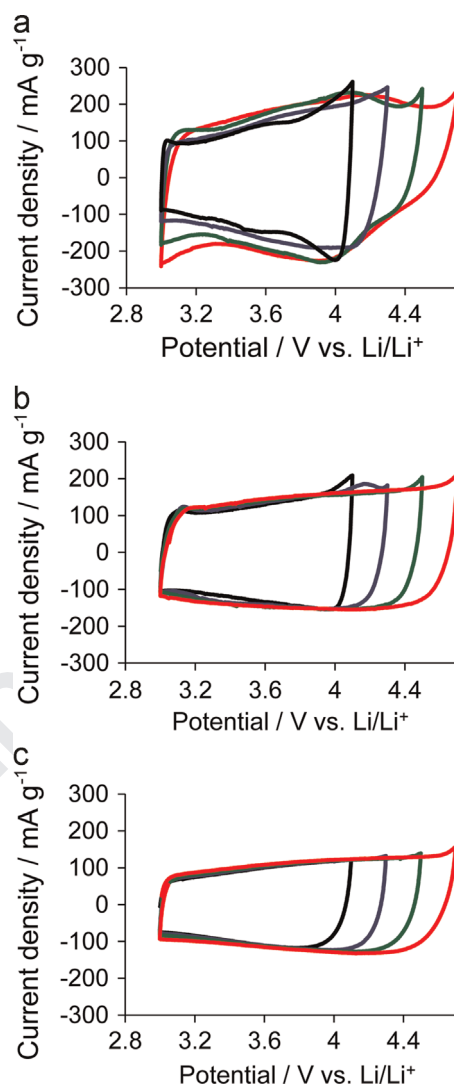


**Fig. 7.** CV patterns (fourth cycle) of (a) ZTC, (b) MSC30, and (c) YP-50F, measured in  $1$  M LiPF<sub>6</sub>/EC+DEC. Scan rate is  $1$  mV s<sup>-1</sup>.

capacitor with the current capacitance level ( $\sim 330$  F g<sup>-1</sup>). Based on the redox mechanism reported in this work, a further effort is desired to achieve much larger pseudocapacitance.

### 3.6. Pseudocapacitance of ZTC in $1$ M LiPF<sub>6</sub>/EC+DEC

Redox-active organic materials (e.g. molecules and polymers) are expected as a positive electrode of rechargeable batteries [25,32–35], and a high redox potential is desired to achieve a high voltage operation of the batteries. Accordingly, the pseudocapacitance of ZTC at a positive potential range by furan-type ether is of interest. Since the proposed redox mechanism (Fig. 4) is based on the reversible conversion of furan into its cation radical, the pseudocapacitance can be expected regardless of the type of anion. We thus examined the electrochemical behavior of ZTC in LiPF<sub>6</sub>/EC+DEC, which is a common organic electrolyte for lithium-ion batteries (LIBs) and lithium-ion capacitors (LICs), and it is compared with those of MSC30 and YP-50F. For each of these carbons, four CV scans were measured at first in the range of  $3.0$  to  $4.1$  V (vs. Li/Li<sup>+</sup>). Then, the upper limit potential was expanded stepwise by  $0.2$  V up to  $4.7$  V with repeating four CV measurements at each of the potential ranges. Fig. 7 shows the fourth CV patterns at each potential range. Like in the case shown in Fig. 1a, the capacitance of ZTC is increased upon expanding the upper

limit potential, and ZTC finally shows broad peaks in a potential range around 3.4–4.4 V. Thus, the pseudocapacitance of ZTC appears in the potential range required for positive electrodes of LIBs and LICs. On the other hand, the activated carbons (MSC30 and YP-50F) never show such a pseudocapacitance in this potential range (Fig. 7b and c), and they show almost constant capacitance regardless of the potential range, like the cases in 1 M Et<sub>4</sub>NBF<sub>4</sub>/PC (Fig. 1b and c). The results shown in Fig. 7 again demonstrate the highly reactive nature of ZTC which is quite unique compared to general activated carbons, and suggest the introduction of redox-active functional groups in a variety of electrolyte solutions.

#### 4. Conclusion

By using ZTC which can be electrochemically oxidized very easily in organic electrolytes, the origin of pseudocapacitance of oxygen-functional groups of carbon was discussed in 1 M Et<sub>4</sub>NBF<sub>4</sub>/PC. The oxidized ZTC shows two different types of redox reactions in positive and negative potential regions, respectively. The former reaction could be the formation of the cation radicals of furan-type ethers, while the latter one is assigned to the anion radicals of quinone-type functional groups. The pseudocapacitance shows a good response against current increase, and it is stable at least for 2000 cycles. Also in 1M LiPF<sub>6</sub>/EC+DEC, which is a common electrolyte for LIBs and LICs, ZTC is electrochemically oxidized and shows a large pseudocapacitance in a positive potential range. Thus, pseudocapacitance derived from oxygen-functional groups of carbon may be useful for electrochemical capacitors, LIBs, and LICs.

#### Q3 Uncited reference

[30].

#### Acknowledgment

We thank Tokyo Sangyo Yoshi Co. Ltd., Kansai Coke and Chemicals Co., Ltd., and Kyraray Chemical Co. Ltd. for kindly supplying separators, MSC30, and YP-50F, respectively. This research was partially supported by the Strategic International Cooperative Program, Japan Science and Technology Agency (T.K.); a Grant-in-Aid for Scientific Research (A), 15H01999 (T.K.); a Grant-in-Aid for Scientific Research (B), 26286020 (H.N.); and the Spanish MINECO, FEDER funds (Project MAT2013-42007-P and PRI-PIBJP-2011-0766). This research was supported also by Nano-Macro Materials, Devices and System Research Alliance and by Network Joint Research Center for Materials and Devices.

#### Appendix A. Supplementary material

Supplementary data associated with this article can be found in the online version at <http://doi:10.1016/j.ensm.2015.08.003>.

#### References

- [1] P. Novak, K. Muller, K.S.V. Santhanam, O. Haas, Electrochemically active polymers for rechargeable batteries, *Chem. Rev.* 97 (1997) 207–281.
- [2] G.A. Snook, P. Kao, A.S. Best, Conducting-polymer-based supercapacitor devices and electrodes, *J. Power Sources* 196 (2011) 1–12.
- [3] K. Nakahara, S. Iwasa, M. Satoh, Y. Morioka, J. Iriyama, M. Suguro, E. Hasegawa, Rechargeable batteries with organic radical cathodes, *Chem. Phys. Lett.* 359 (2002) 351–354.
- [4] M. Yao, H. Senoh, T. Sakai, T. Kiyobayashi, Redox active poly(N-vinylcarbazole) for use in rechargeable lithium batteries, *J. Power Sources* 202 (2012) 364–368.
- [5] S. Isikli, R. Diaz, Substrate-dependent performance of supercapacitors based on an organic redox couple impregnated on carbon, *J. Power Sources* 206 (2012) 53–58.
- [6] Y. Hanyu, I. Honma, Rechargeable quasi-solid state lithium battery with organic crystalline cathode, *Sci. Rep.* 2 (2012) 453.
- [7] S. Isikli, M. Lecea, M. Ribagorda, M.C. Carreño, R. Díaz, Influence of quinone grafting via Friedel–Crafts reaction on carbon porous structure and supercapacitor performance, *Carbon* 66 (2014) 654–661.
- [8] T. Brousse, M. Toupin, R. Dugas, L. Athouel, O. Crosnier, D. Belanger, Crystalline MnO<sub>2</sub> as possible alternatives to amorphous compounds in electrochemical supercapacitors, *J. Electrochem. Soc.* 153 (2006) A2171–A2180.
- [9] N.L. Wu, Nanocrystalline oxide supercapacitors, *Mater. Chem. Phys.* 75 (2002) 6–11.
- [10] Z.X. Ma, T. Kyotani, A. Tomita, Preparation of a high surface area microporous carbon having the structural regularity of Y zeolite, *Chem. Commun.* (2000) 2365–2366.
- [11] H. Nishihara, T. Kyotani, Templated nanocarbons for energy storage, *Adv. Mater.* 24 (2012) 4473–4498.
- [12] R. Berenguer, H. Nishihara, H. Itoi, T. Ishii, E. Morallon, D. Cazorla-Amoros, T. Kyotani, Electrochemical generation of oxygen-containing groups in an ordered microporous zeolite-templated carbon, *Carbon* 54 (2013) 94–104.
- [13] H. Itoi, H. Nishihara, T. Ishii, K. Nueangnoraj, R. Berenguer-Betrian, T. Kyotani, Large pseudocapacitance in quinone-functionalized zeolite-templated carbon, *Bull. Chem. Soc. Jpn.* 87 (2014) 250–257.
- [14] H. Itoi, H. Nishihara, T. Kogure, T. Kyotani, Three-dimensionally arrayed and mutually connected 1.2-nm nanopores for high-performance electric double layer capacitor, *J. Am. Chem. Soc.* 133 (2011) 1165–1167.
- [15] T. Ishii, S. Kashihara, Y. Hoshikawa, J.-i. Ozaki, N. Kannari, K. Takai, T. Enoki, T. Kyotani, A quantitative analysis of carbon edge sites and an estimation of graphene sheet size in high-temperature treated, non-porous carbons, *Carbon* 80 (2014) 135–145.
- [16] G. Eggert, J. Heitbaum, Electrochemical reactions of propylenecarbonate and electrolytes solved therein – A DEMS study, *Electrochim. Acta* 31 (1986) 1443–1448.
- [17] M.J. Bleda-Martinez, J.A. Macia-Agullo, D. Lozano-Castello, E. Morallon, D. Cazorla-Amoros, A. Linares-Solano, Role of surface chemistry on electric double layer capacitance of carbon materials, *Carbon* 43 (2005) 2677–2684.
- [18] J.L. Figueiredo, M.F.R. Pereira, M.M.A. Freitas, J.J.M. Orfao, Modification of the surface chemistry of activated carbons, *Carbon* 37 (1999) 1379–1389.
- [19] G.E. Romanos, V. Likodimos, R.R.N. Marques, T.A. Steriotes, S.K. Papageorgiou, J. L. Faria, J.L. Figueiredo, A.M.T. Silva, P. Falaras, Controlling and quantifying oxygen functionalities on hydrothermally and thermally treated single-wall carbon nanotubes, *J. Phys. Chem. C* 115 (2011) 8534–8546.
- [20] D. Cazorla-Amorós, D. Lozano-Castelló, E. Morallón, M.J. Bleda-Martínez, A. Linares-Solano, S. Shiraishi, Measuring cycle efficiency and capacitance of chemically activated carbons in propylene carbonate, *Carbon* 48 (2010) 1451–1456.
- [21] D. Hulicova, J. Yamashita, Y. Soneda, H. Hatori, M. Kodama, Supercapacitors prepared from melamine-based carbon, *Chem. Mater.* 17 (2005) 1241–1247.
- [22] T. Kwon, H. Nishihara, H. Itoi, Q.H. Yang, T. Kyotani, Enhancement mechanism of electrochemical capacitance in nitrogen-/boron-doped carbons with uniform straight nanochannels, *Langmuir* 25 (2009) 11961–11968.
- [23] M. Kodama, J. Yamashita, Y. Soneda, H. Hatori, K. Kamegawa, Preparation and electrochemical characteristics of N-enriched carbon foam, *Carbon* 45 (2007) 1105–1107.
- [24] V.J. Koshy, V. Swayambunathan, N. Periasamy, A reversible redox couple in quinone-hydroquinone system in non-aqueous medium, *J. Electrochem. Soc.* 127 (1980) 2761–2763.
- [25] T. Nokami, T. Matsuo, Y. Inatomi, N. Hojo, T. Tsukagoshi, H. Yoshizawa, A. Shimizu, H. Kuramoto, K. Komae, H. Tsuyama, J. Yoshida, Polymer-bound pyrene-4,5,9,10-tetraone for fast-charge and -discharge lithium-ion batteries with high capacity, *J. Am. Chem. Soc.* 134 (2012) 19694–19700.
- [26] C. Frontana, A. Vazquez-Mayagoitia, J. Garza, R. Vargas, I. Gonzalez, Substituent effect on a family of quinones in aprotic solvents: an experimental and theoretical approach, *J. Phys. Chem. A* 110 (2006) 9411–9419.
- [27] P.E. Fanning, M.A. Vannice, A DRIFTS study of the formation of surface groups on carbon by oxidation, *Carbon* 31 (1993) 721–730.
- [28] U. Zielke, K.J. Huttinger, W.P. Hoffman, Surface-oxidized carbon fibers 1. Surface structure and chemistry, *Carbon* 34 (1996) 983–998.
- [29] M.C. Pham, P.C. Lacaze, Study of the redox process of poly(2-naphthol) film using in-situ multiple internal-reflection FTIR spectroscopy, *J. Electrochem. Soc.* 141 (1994) 156–160.
- [30] H. Nishihara, Q.H. Yang, P.X. Hou, M. Unno, S. Yamauchi, R. Saito, J.I. Paredes, A. Martinez-Alonso, J.M.D. Tascon, Y. Sato, M. Terauchi, T. Kyotani, A possible buckybowllike structure of zeolite templated carbon, *Carbon* 47 (2009) 1220–1230.
- [31] B. Piro, E.A. Bazzouai, M.C. Pham, P. Novak, O. Haas, Multiple internal reflection FTIR spectroscopic (MIRFTIRS) study of the redox process of poly(5-amino-1,4-



- 1 naphthoquinone) film in aqueous and organic media, *Electrochim. Acta* 44  
2 (1999) 1953–1964.
- 3 [32] T. Tomai, S. Mitani, D. Komatsu, Y. Kawaguchi, I. Honma, Metal-free aqueous  
4 redox capacitor via proton rocking-chair system in an organic-based couple,  
5 *Sci. Rep.* 4 (2014) 3591.
- 6 [33] Z.P. Song, H. Zhan, Y.H. Zhou, Anthraquinone based polymer as high perfor-  
7 mance cathode material for rechargeable lithium batteries, *Chem. Commun.*  
8 (2009) 448–450.
- 9
- 10
- 11
- 12
- 13
- 14
- 15
- 16
- 17
- 18
- 19
- 20
- 21
- 22
- 23
- 24
- 25
- 26
- 27
- 28
- 29
- 30
- 31
- 32
- 33
- 34
- 35
- 36
- 37
- 38
- 39
- 40
- 41
- 42
- 43
- 44
- 45
- 46
- 47
- 48
- 49
- 50
- 51
- 52
- 53
- 54
- 55
- 56
- 57
- 58
- 59
- 60
- 61
- 62
- 63
- 64
- 65
- 66
- [34] K.M. Ismail, Z.M. Khalifa, M.A. Azzem, W.A. Badawy, Electrochemical pre-  
67 paration and characterization of poly(1-amino-9,10-anthraquinone) films,  
68 *Electrochim. Acta* 47 (2002) 1867–1873.
- [35] M. Yao, H. Senoh, S.-i Yamazaki, Z. Siroma, T. Sakai, K. Yasuda, High-capacity  
69 organic positive-electrode material based on a benzoquinone derivative for  
70 use in rechargeable lithium batteries, *J. Power Sources* 195 (2010) 8336–8340.  
71  
72  
73  
74  
75  
76  
77  
78  
79  
80  
81  
82  
83  
84  
85  
86  
87  
88  
89  
90  
91  
92  
93  
94  
95  
96  
97  
98  
99  
100  
101  
102  
103  
104  
105  
106  
107  
108  
109  
110  
111  
112  
113  
114  
115  
116  
117  
118  
119  
120  
121  
122  
123  
124  
125  
126  
127  
128  
129  
130  
131  
132